JOURNAL OF ELECTROMAGNETIC ENGINEERING AND SCIENCE, VOL. 24, NO. 2, 109~119, MAR. 2024

https://doi.org/10.26866/jees.2024.2.r.210
ISSN 2671-7263 (Online) · ISSN 2671-7255 (Print)

Four-Element Biodegradable Substrate-Integrated MIMO DRA with Radiation Diversity

Rasika Verma · Rohit Sharma*

Abstract

This article presents a four-element directional multiple input multiple output (MIMO) rectangular dielectric resonator antenna (RDRA) equipped with strategically placed copper reflector plates to enhance port isolation. This design aims to achieve an extended coverage range without compromising the coverage area. The proposed MIMO antenna is 3D printed using biodegradable polylactic acid to ensure mechanical robustness and then integrated with the substrate to prevent mis-mounting issues. The proposed design exhibits good MIMO characteristics, registering a 3-GHz bandwidth (4–7 GHz) for $|S_{11}| \leq -10$ dB and a minimum radiation gain of 7 dBi for all four RDRAs. The antenna demonstrates a rotation of radiation patterns for different ports, thus enabling beam formation in specific directions. With a beam width of 71.2°, the antenna covers all directions without any fade zones. The proposed 3D printed antenna offers simplicity, strong MIMO properties, and practicality for wireless communication systems, making it suitable for industrial, scientific, and medical band applications.

Key Words: DRA (Dielectric Resonator Antenna), ISM (Industrial, Scientific, and Medical), MIMO (Multiple Input Multiple Output), RDRA (Rectangular DRA).

I. Introduction

The escalating demand for antennas with high data transmission rates and broad coverage extents is closely aligned with the prevailing trajectory of electronics towards wireless and automation paradigms. Nevertheless, while the advent of conventional coaxial antennas ostensibly met the initial requisites, the swift recognition of their limitation in confining signal propagation to short ranges precipitated a paradigm shift in favor of directed antennas. Subsequently, a novel challenge emerged—the curtailed radial coverage that is intrinsic to directed antennas. To mitigate this challenge, a mechanical motor was introduced to facilitate rotational adjustments [1]. However, this measure incurred a substantial increase in the system's overall mass, consequently impeding its efficacy. This was a result of the inherent lethargy of mechanical rotations, which paled in comparison to the rapidity of electrical switching mechanisms. In response, a multiple input multiple output (MIMO) antenna configuration emerged as a potential solution to this shortcoming, overcoming the constraints of its predecessors. In the current study, the proposed MIMO architecture entails the integration of four coaxially fed directional dielectric resonator antennas (DRAs), each radiating in alignment with the azimuth plane's four cardinal directions. As a result, the aggregate gain is uniformly bolstered across all spatial orientations.

MIMO employs many ports, some of which serve as the

Manuscript received May 20, 2023 ; Revised September 02, 2023 ; Accepted October 30, 2023. (ID No. 20230520-094J)
Department of Electronics and Communication, SRM Institute of Science and Technology, Ghaziabad, India.
*Corresponding Author: Rohit Sharma (e-mail: rasikaverma21@gmail.com)

transmitter (Tx) while others perform the role of the receiver (Rx), to maximize the data transfer rate while also minimizing mistakes [2]. This method is adaptable and can be utilized in a variety of ways, such as by employing single antennas with various feeds or many antennas on a single substrate. Notably, these two methods are also the ones that are implemented most frequently. However, both are characterized by drawbacks related to isolating the ports. To address this challenge, extensive research has been conducted to increase the isolation between ports by, for instance, creating hybrid feeding mechanisms for the generation of orthogonal modes [3–6], using metallic elements as parasitic structures [7], employing metasurface shields [8], and using frequency selective surfaces (FSSs) [9] to reduce the displacement current between ports.

Over the past few decades, DRAs have received substantial research attention. Notably, they are volumetric structures built using non-conductive low-loss dielectric materials. Several forms of DRAs have been proposed in the open literature, including cylindrical, rectangular, hemispherical, and triangular DRAs, among others. DRAs are growing in popularity in the research community, primarily due to their several advantages over planar microstrip antennas, such as wider impedance bandwidth, low loss, convenience of excitation, and so on [10–13]. Moreover, compared to planar antennas, DRAs possess a more flexible design due to their volumetric nature.

The volumetric nature of DRAs also enables the efficient utilization of available space. Their compact and three-dimensional (3D) form factor allows for the integration of multiple antenna elements, thus facilitating the implementation of MIMO systems and beamforming techniques. Such arrangements significantly enhance the antenna's capacity to support multiple data streams, improve communication link performance, and enhance system reliability. Additionally, the volumetric nature of DRAs enables the exploration of various dielectric materials characterized by diverse permittivity and loss tangents, ultimately offering enhanced control over antenna characteristics, including bandwidth, efficiency, and directivity. This versatility further encourages the adaptation of the antenna to different operating environments and the optimization of its performance to suit specific user requirements.

With increasing electronic production over the years, the crisis involving dangerous e-waste is worsening [14]. Under such circumstances, adopting a biodegradable polymer can remedy the e-waste problem without hindering market expansion. During its lifespan, a biodegradable substance does not deteriorate [15], but it degrades on using particular techniques under specific circumstances. It breaks down into biomass, inorganic chemicals, and water (H_2O), carbon dioxide (CO_2), or methane (CH_4) when it comes in contact with naturally existing microbes, such as bacteria, fungus, and algae [16]. Notably, to create bio-based polymers, renewable resources, such as corn, potato, rice, soya, sugarcane, wheat, and vegetable oil, are used. Polylactic acid (PLA) is one such popular bio-based polymer material that is used in 3D printers and is widely accessible as 3D printable filaments.

Biodegradable plastics are among the most promising alternatives to traditional petroleum-based plastics, which have several negative environmental effects—pollution of land, water, and air, as well as global warming. Among the various biodegradable plastics available, PLA is not only widely available but can also be safely used and thereafter destroyed without harming the environment [17]. Furthermore, in terms of the several qualities necessary for industrial use—be it mechanical, physical, and electrical properties or biocompatibility and processability—PLA is similar to other common polymers, such as polypropylene and polyethylene terephthalate. Due to its unique properties, PLA has emerged as the most widely used biopolymer in a variety of sectors, including the electronics, packaging, agriculture, automotive, and medical industries. Therefore, owing to its attractive traits, the proposed design uses PLA as the dielectric material for the antenna. Additionally, as a form of additive manufacturing, 3D printing is employed to efficiently create the antenna, layer by layer, with extremely high accuracy. In this context, the literature has already established that complex antenna shapes are achievable using 3D printing [18, 19].

This article proposes a four-port MIMO DRA with copper backing for Wi-Fi, WiMax, and 5G applications. It is designed using PLA as the dielectric material, which is printed alongside the substrate to reduce the dielectric resonator (DR) mounting error and feed error, considering that the feeding pin holes are already present in the printed structure. Furthermore, the complete assembly is printed in its entirety, thus increasing its mechanical strength. To achieve high gain and a wide bandwidth, several parameters, such as pin height, DRA position, and copper backing height, were examined. Moreover, the proposed antenna bears a simple design and can be constructed easily.

II. Antenna Geometry

Fig. 1 depicts the fundamental rectangular dielectric resonator antennas (RDRAs) that comprise the proposed MIMO antenna. Each RDRA is 26 mm tall (H_D), 15 mm wide (W_D), and 26 mm long (L_D). Furthermore, each DRA is covered with a reflective copper layer having the following dimensions: length (L_C) = 14 mm, width (W_C) = 0.1 mm, and height (H_C) = 26 mm. Each DRA is separated from the others by a DRA_{GAP} of 19 mm fed through coaxial cables. The pin height within each DRA (H_P) is 10 mm, while the distance between each pin and its corresponding copper plate is 13.5 mm (CP_{GAP}).

This DRA assembly was mounted on a PLA (ε_r = 3.47 and tanδ = 0.005) substrate with length (L_S), width (W_S), and height (H_S) of 80 mm, 80 mm, and 0.8 mm, respectively. The ground

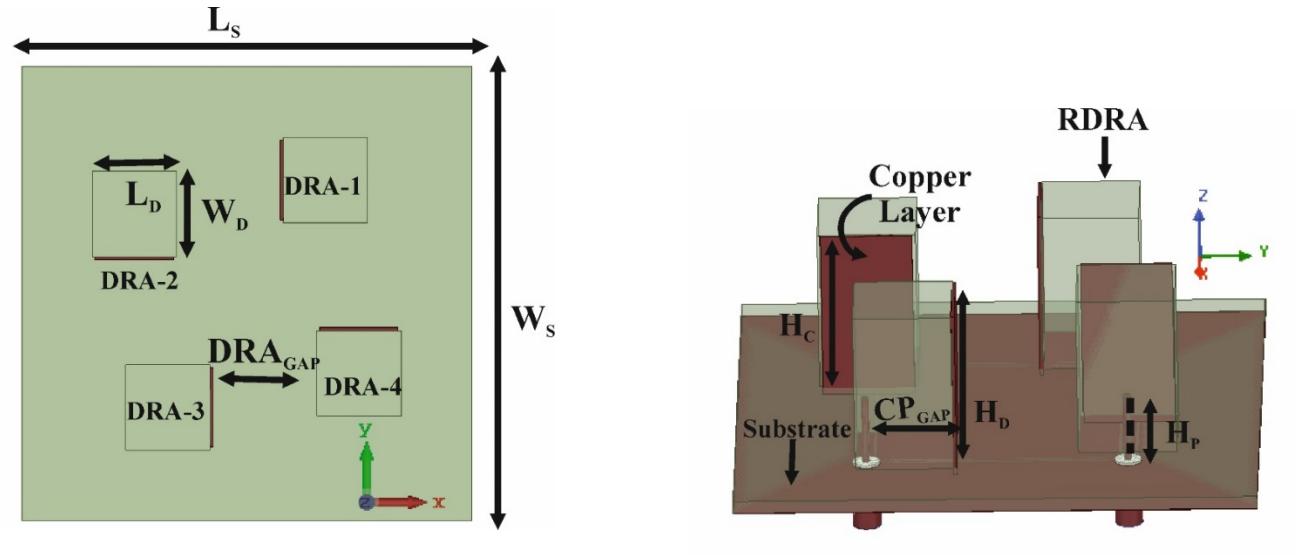

(a) (b)

Fig. 1. MIMO antenna geometry: (a) top view and (b) side view.

plane, made of copper, had the following dimensions: length (L_G) = width (W_G) = L_S = 80 mm and thickness = 0.035 mm.

To ensure simple fabrication, the entire DRA and substrate assembly was 3D printed.

III. Parametric Studies

To attain the best outcome that meets the needs of the proposed project, several DRA parameters were examined at various levels. A few of these parametric studies are described below.

1. Pin Height Parametric Study

The DRs, with dimensions of L = 15 mm, W = 15 mm, and H = 26 mm, were initially placed on the substrate (80 mm × 80 mm × 0.8 mm). They were spaced apart by a DRA_{GAP} of 25 mm and a CP_{GAP} of 7.5 mm. Notably, the theoretical formula for obtaining the resonant frequency (f_r) of an RDRA can be expressed as follows:

$$f_r = \frac{c}{2\pi\sqrt{\varepsilon_r}}\sqrt{k_x^2 + k_y^2 + k_z^2}, \quad (1)$$

where ε_r is the dielectric constant of the DRs, c is the speed of light in free space, and the symbols k_x, k_y, and k_z represent the wave numbers in the *x*, *y*, and *z* directions, respectively.

To boost the resonance frequency and bandwidth, the feeding pin height parameter was considered. According to the simulated findings presented in Fig. 2, at a pin height (H_P) of 10 mm, it is possible to effectively create a band of 3 GHz for $|S_{11}|$ −10 dB, or from 4 GHz to 7 GHz, with the reflection coefficient ($|S_{11}|$) dropping as low as −14 dB.

The *S*-parameters are presented separately in Fig. 2 as three graphs to simplify the comprehension of the results.

- Since $|S_{11}|$, $|S_{22}|$, $|S_{33}|$, and $|S_{44}|$ are identical due to their electric symmetry, the reflection coefficients of the same ports, i.e., $|S_{11}|$, $|S_{22}|$, $|S_{33}|$, and $|S_{44}|$, are presented in the context of only $|S_{11}|$ in Fig. 2(a).
- Similarly, since the electric symmetricity of $|S_{21}|$, $|S_{32}|$, $|S_{43}|$, and $|S_{14}|$ are identical, isolation between the adjacent ports, i.e., $|S_{21}|$, $|S_{32}|$, $|S_{43}|$ and $|S_{14}|$, are shown in the context of only $|S_{21}|$ in Fig. 2(b).
- Isolation between opposing ports, such as $|S_{31}|$ and $|S_{42}|$, is depicted with regard to only $|S_{31}|$ in Fig. 2(c).

However, this MIMO antenna design exhibited deficiencies in some key parameters, such as directivity, gain, and other crucial properties, including mutual coupling, rendering it unsuitable for practical real-world use. The performance evaluation of the antenna considered various metrics, such as the correlation coefficient (ρ) presented in Fig. 3(a), diversity gain (G_{app}) in Fig. 3(b), directivity in Fig. 3(c), and gain in Fig. 3(d). These figures provide a comprehensive overview of the antenna's operational characteristics and limitations.

It is evident that despite achieving impedance matching, the other vital variables failed to meet the required standards. To ensure effective MIMO operation, it is imperative to ascertain critical MIMO system characteristics (such as the correlation coefficient and diversity gain) that significantly influence the system's capacity to exploit spatial channel diversity.

As depicted in Fig. 3(a) and 3(b), an inverse relationship was observed between the correlation coefficient and the diversity gain, indicating that a lower correlation value maximized system diversity. A lower correlation coefficient signifies reduced interchannel dependency, which enhances the MIMO system's ability to leverage independent transmission pathways, thereby improving overall performance.

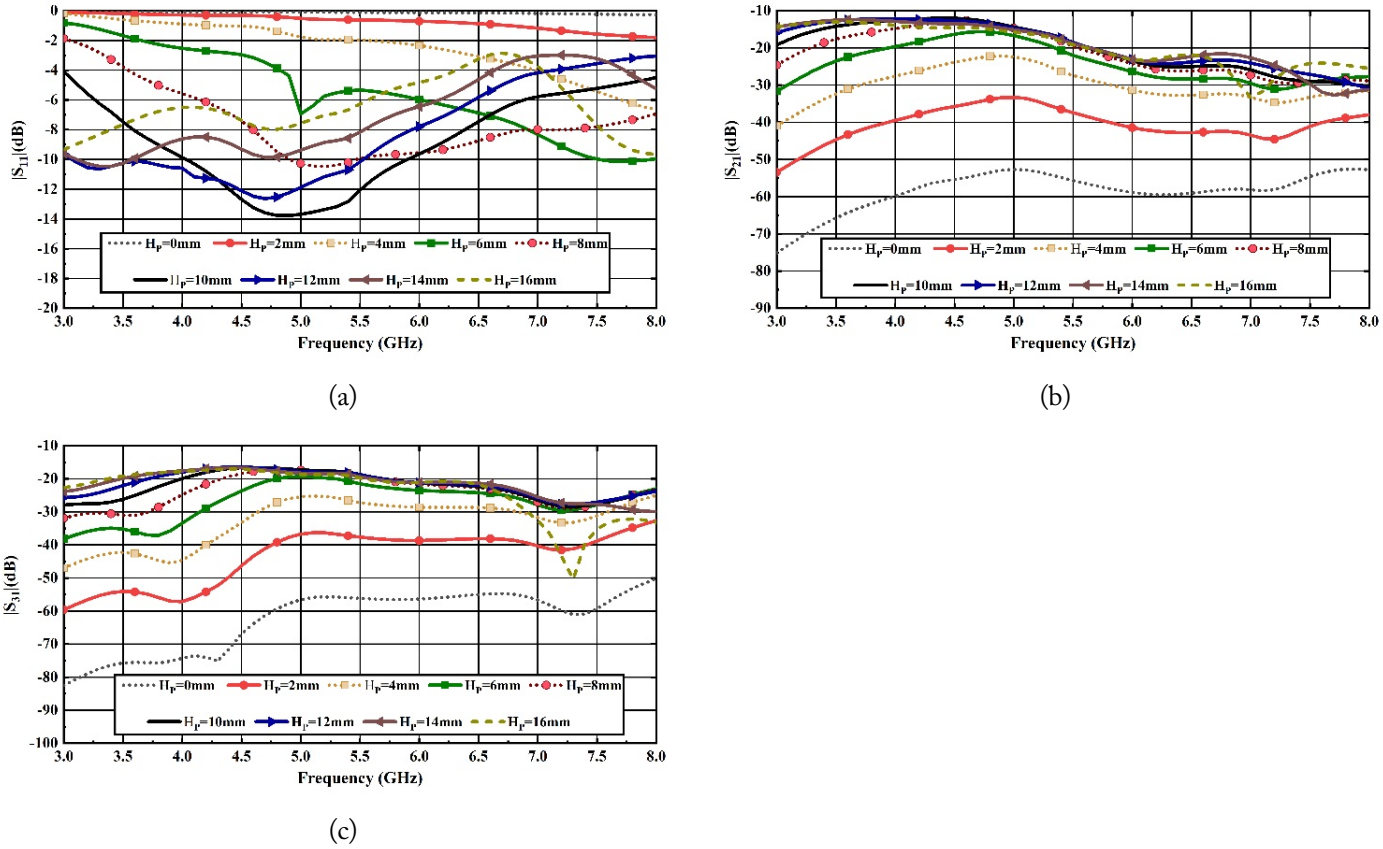

Fig. 2. *S*-parameters for variations in the feed pin height (H_P): (a) S_{11}, (b) S_{21}, and (c) S_{31}.

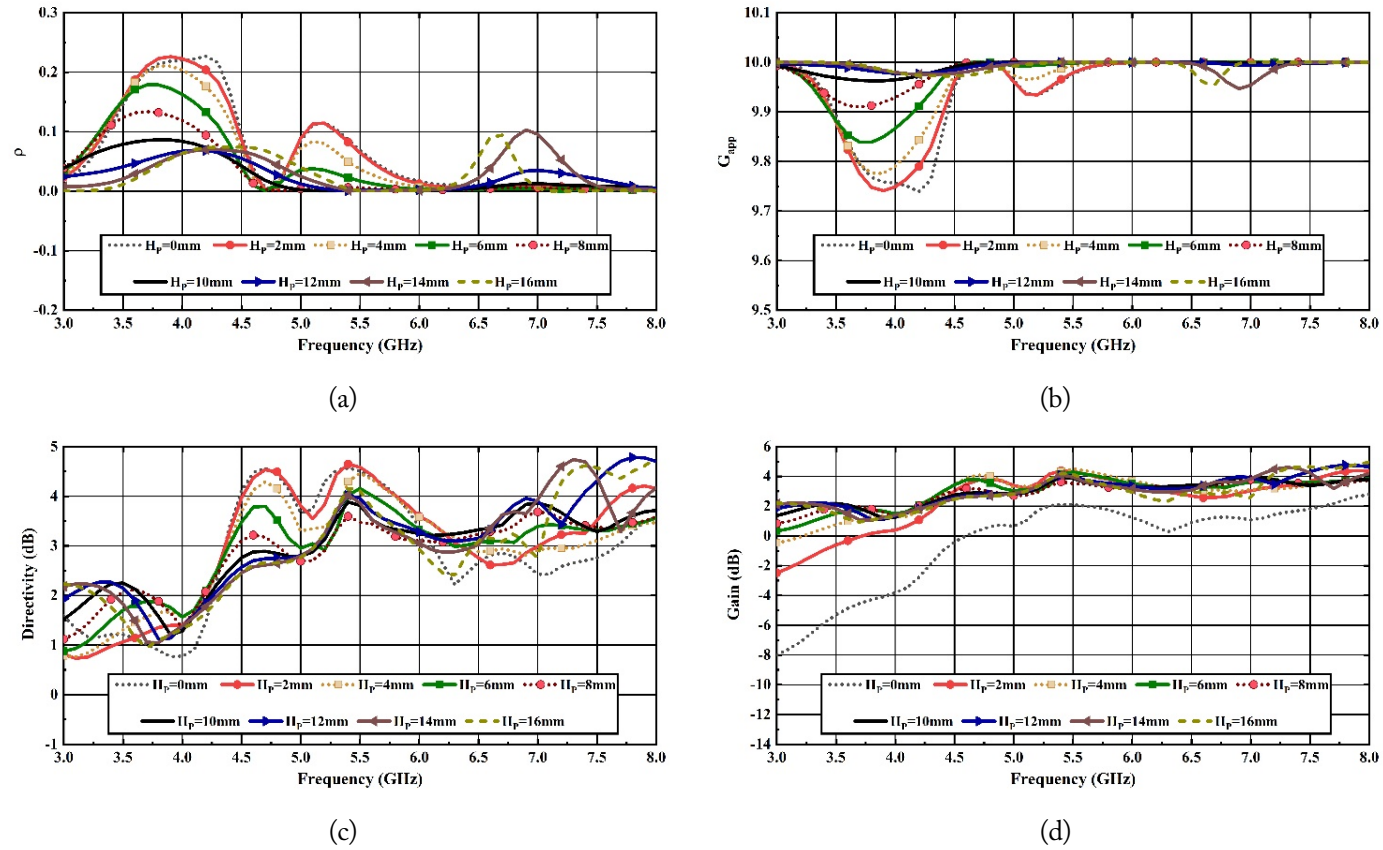

Fig. 3. Antenna parameters for variations in the feed pin height (H_P): (a) correlation coefficient (ρ), (b) diversity gain (G_{app}), (c) directivity, and (d) gain.

Careful evaluation and optimization of these crucial factors played a pivotal role in enhancing the performance of the proposed MIMO antenna. By reducing the correlation coefficient and increasing the diversity gain, the antenna's total efficiency was improved, and its compatibility with reliable and effective MIMO communication systems was ensured. It was evident that achieving the desired antenna characteristics and meeting the specific performance requirements for MIMO applications demanded a methodical and precise approach incorporating cutting-edge design methodologies and sophisticated simulations.

The following formula demonstrates the mathematical relationship between the correlation coefficient (ρ) and diversity gain (G_{app}):

$$G_{app} = 10 * \sqrt{1 - |\rho|^2}. \quad (2)$$

The observed values of $\rho \approx 0.1$ and $G_{app} < 10$ within certain ranges of the operation signified inadequate MIMO performance, posing concerns about the overall efficiency of the system. Additionally, both directivity and gain were below the threshold of 4 dB, further compounding the apprehensions surrounding the antenna's effectiveness.

However, these issues were successfully addressed by implementing a copper layer as a reflector, as elaborated in the next section. The introduction of the copper reflector proved to be a pivotal solution in overcoming the above-mentioned shortcomings and significantly improving the performance of the MIMO antenna. By leveraging the benefits of the copper reflector, effective improvements in directivity, gain, and other critical parameters were achieved, thereby elevating the antenna's overall capabilities to meet the required performance standards for MIMO applications. The next section delves into the specifics of this innovative solution, shedding light on the intricate design considerations and demonstrating its positive impact on the antenna's performance metrics.

2. Copper Backing Height Parametric Study

The second phase of the experimental process attempted to solve the various issues identified in the initial design, such as inadequate MIMO parameters, low directivity, and inadequate gain of the DRAs. To surmount these obstacles, a copper coating was applied to the walls of the DRAs, focusing especially on the wall coupling with the other DRAs. Interestingly, this led to an improvement in isolation, but it distorted the impedance matching, as concluded by examining the S_{11} in Fig. 4(a), S_{21} in Fig. 4(b), and S_{31} in Fig. 4(c). It was found that a copper coating height (H_C) of 26 mm yielded the most favorable results for the intended objective of isolation, effectively mitigating previously identified deficiencies.

Copper is a highly conductive material that improves the

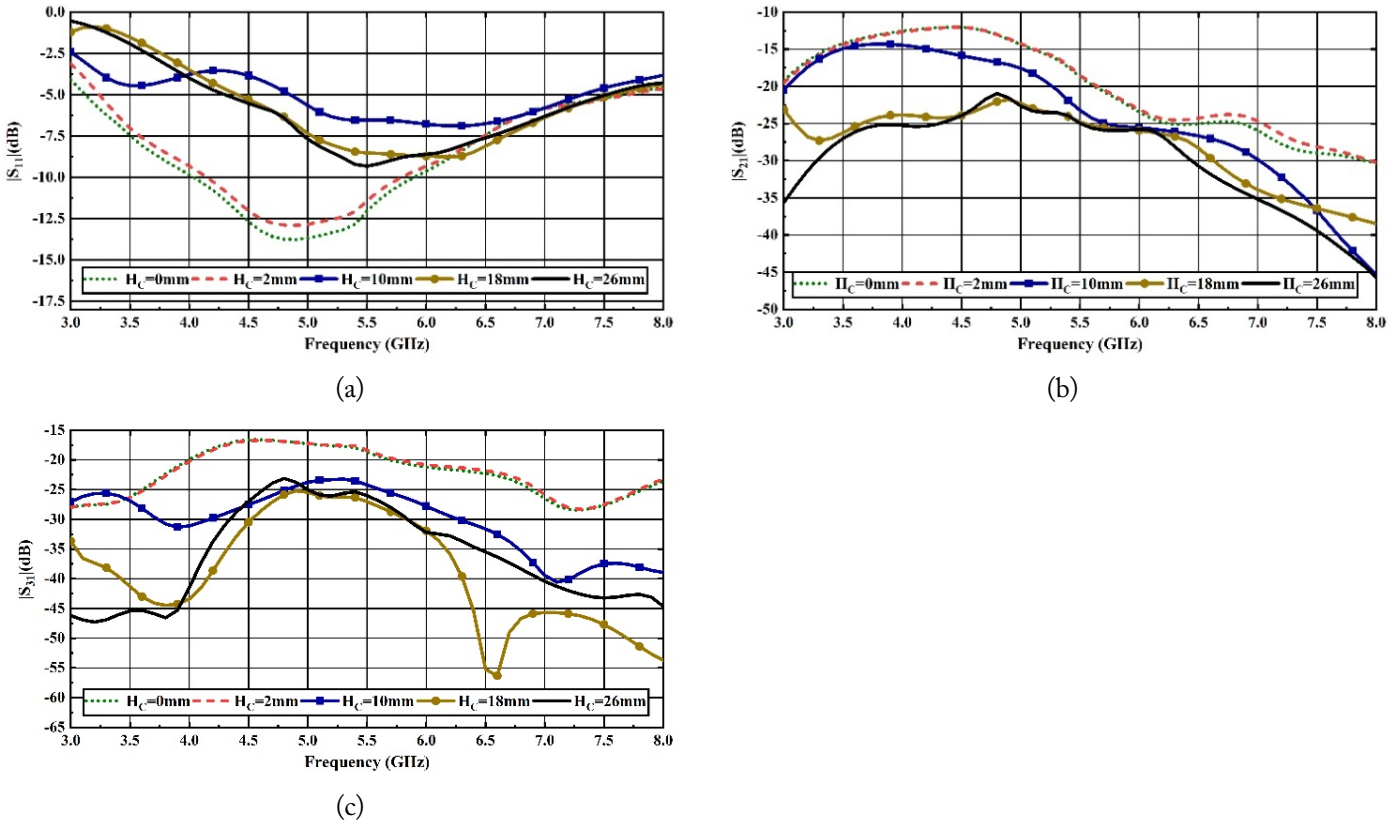

Fig. 4. Parametric results for variations in the height of the copper plate: (a) S_{11}, (b) S_{21}, and (c) S_{31}.

electromagnetic efficacy of antennas. Therefore, by applying a copper coating to the wall responsible for mutual coupling, the coupling effects between adjacent DRAs can be decreased. This, in turn, reduces signal interference and crosstalk, resulting in enhanced isolation between antenna elements.

In addition, the copper coating served as a highly effective reflector—redirecting and concentrating the radiated energy in the desired direction. As depicted in Fig. 5(a) and 5(b), the directivity and gain of the DRAs improved substantially, resulting in an overall performance enhancement of the antenna system. Furthermore, Fig. 5(c) and 5(d) show that the correlation coefficient (ρ) and diversity gain (G_{app}) exhibited identical patterns.

The next section focuses on addressing the impedance mismatch by improving DRA locations while retaining the copper backing. It attempts to achieve the coexistence of optimal impedance matching and improved isolation by maximizing the individual and group performances of the DRAs through their strategic placement, resulting in better $|S_{11}|$ values.

3. Parametric Study of the DRA Position with Copper Backing

While the introduction of copper coating resulted in a degradation in impedance matching, it was effectively addressed by strategically relocating the DRAs. Through careful investigation, it was observed that impedance matching improved consistently as the feed pin-to-copper plating gap (CP_{GAP}) widened, with the best performance achieved at CP_{GAP} = 13.5 mm, offering a bandwidth of 3 GHz.

Fig. 6(a) illustrates the improved impedance matching achieved at a CP_{GAP} of 13.5 mm. Remarkably, these enhancements were achieved while maintaining a low level of mutual coupling between the DRAs, as evident in Fig. 6(b) and 6(c), which depict scattering parameters S_{21} and S_{31}, respectively.

The next section presents a comprehensive analysis of the antenna system's radiation patterns, directivity, gain, envelope correlation coefficient (ECC), and diversity gain. In addition, it provides the measured data for validating the performance enhancements achieved by the optimized DRA positions and the corresponding CP_{GAP}, thereby enhancing comprehension and appreciation of the research outcomes of this study.

IV. Results and Comparison

After the successful creation of a prototype, the performance of the proposed four-port MIMO DRA with radiation diversity was meticulously evaluated. The fabricated model of the prototype antenna is depicted in Fig. 7, while the exhaustive results of the simulations and measurements of the *S*-parameters for the proposed design are illustrated in Fig. 8.

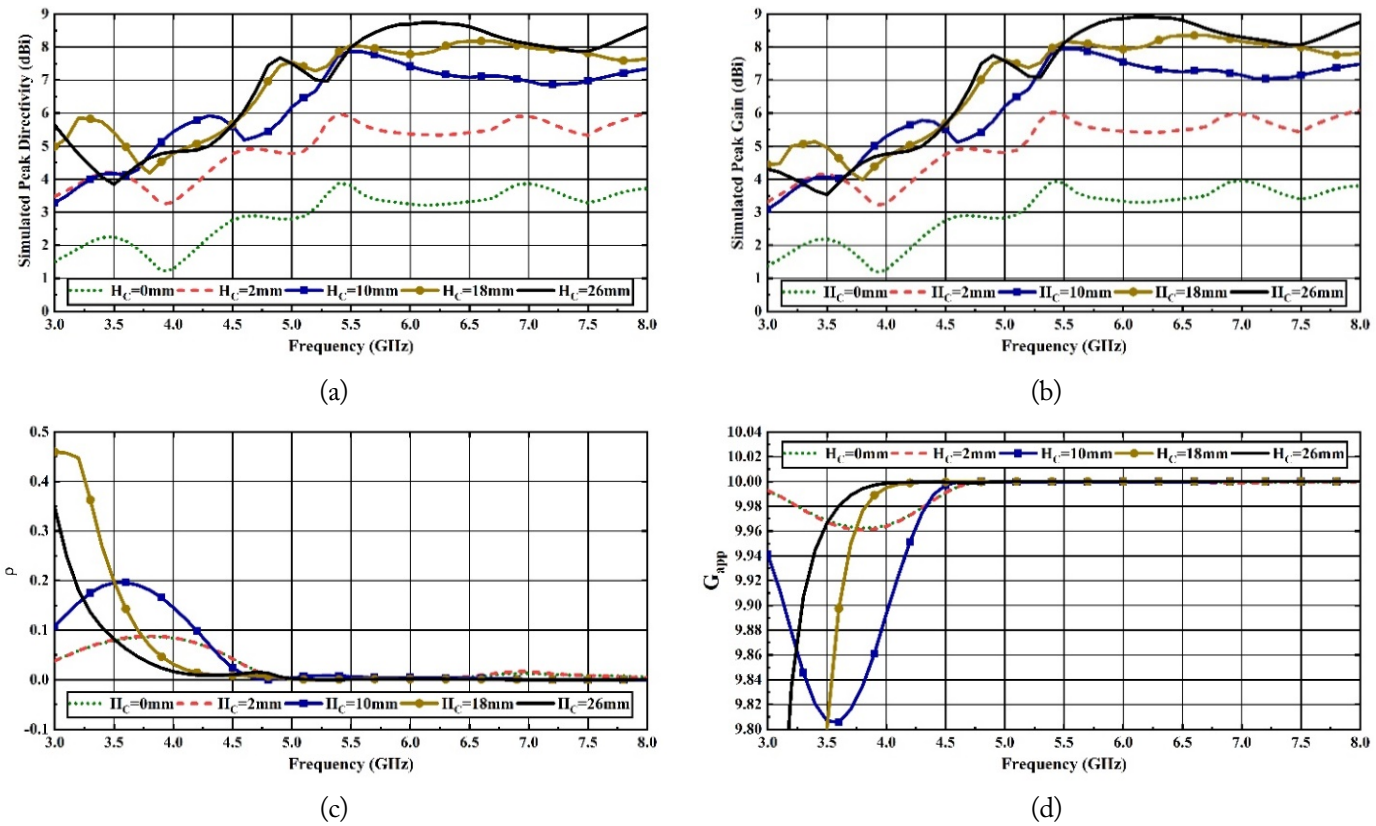

Fig. 5. Antenna parameters for variations in the copper backing height (H_C): (a) peak directivity (ρ), (b) peak gain, (c) correlation coefficient, and (d) diversity gain (G_{app}).

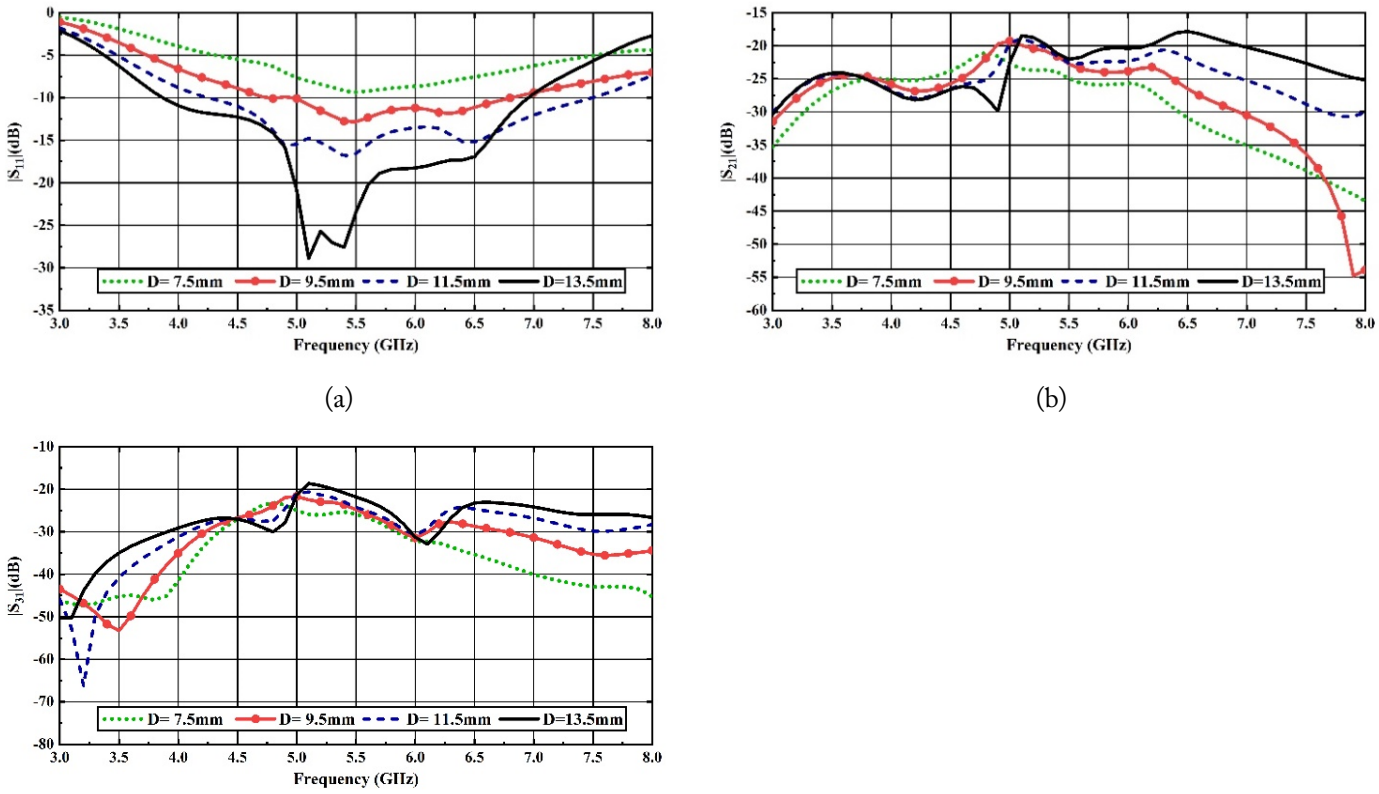

Fig. 6. *S*-parameters for different variations of the DRA position: (a) S_{11}, (b) S_{21}, and (c) S_{31}.

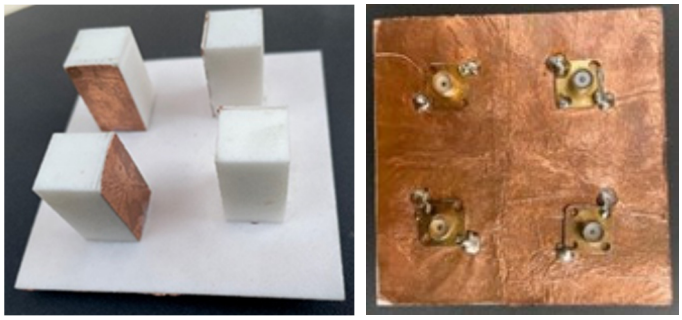

Fig. 7. Fabricated model of proposed antenna: (a) front view and (b) back view.

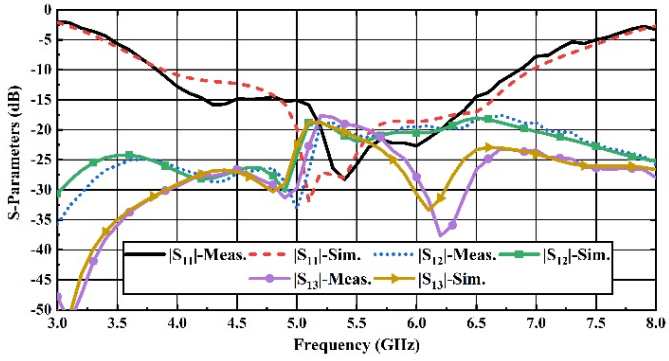

Fig. 8. Simulated and measured *S*-parameters of the proposed DRA.

The high level of agreement between the simulated and measured results within the frequency ranges of interest—ranging from 3.6 GHz to 6.6 GHz and encompassing a significant portion of the ISM band—makes the proposed MIMO antenna an ideal candidate for modern Wi-Fi, Bluetooth, and other Internet-of-Things devices where the ISM band is crucial. Notably, the copper coating used within the operational bandwidth effectively reduced mutual coupling between ports, resulting in a 20 dB isolation between ports.

In addition to the aforementioned analyses, Fig. 9 depicts the measured and simulated gain and directivity of the MIMO antenna. The MIMO antenna achieved a peak gain of approximately 8 dBi at 5.4 GHz—its resonant frequency (measured). These results offer crucial insights into the antenna's radiation characteristics, thus bolstering the design's efficacy and viability for a variety of real-world applications.

In addition to isolation, other critical antenna properties, such as the correlation coefficient (ρ) and diversity gain (G_{app}), also had a substantial impact on the MIMO antenna's overall performance. As shown in Fig. 10, both the simulated and measured c oefficients of correlation (ρ) remained astonishingly low—below 0.001—indicating robust isolation between ports over the entire operating frequency range. Similarly, the diversity gain (G_{app}) consistently maintained a value of 10 across the spectrum, further validating the robust isolation between the antenna's terminals.

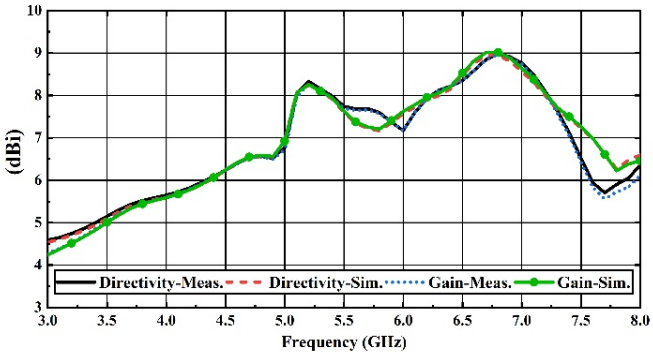

Fig. 9. Comparison of the simulated and measured directivity and gain of the proposed DRA.

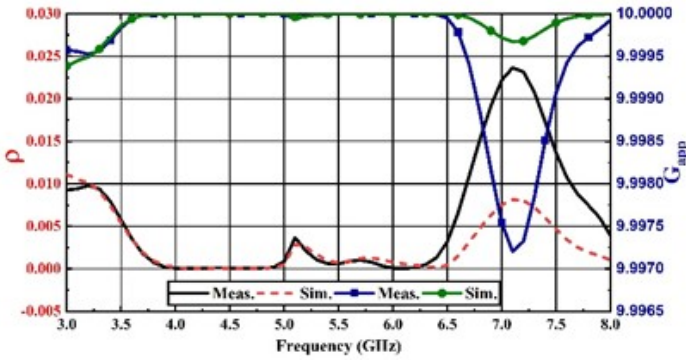

Fig. 10. Comparison of the simulated and measured correlation coefficient and diversity gain of the proposed DRA.

Fig. 11 compares the simulated and measured normalized radiation patterns at the resonant frequency, indicating the particular direction in which the beam forms when the antenna operates from the different ports. For instance, in the case of Port-1, the radiation is in the +X direction, i.e., $\phi = 0^{\circ}$, $\theta = 45^{\circ}$, whereas for Port-2, the radiation is in the +Y direction, i.e., $\phi = 90^{\circ}$, $\theta = 45^{\circ}$. Furthermore, the radiation beam shifts to $\phi = 180^{\circ}$, $\theta = 45^{\circ}$ when Port-3 is active, while Port-4 focuses the beam toward $\phi = 270^{\circ}$, $\theta = 45^{\circ}$.

The radiation patterns evidently indicate the direction in which the primary beam of the antenna is formed. Notably, the beam width, which measures 71.2°, ensures wide coverage without any fade zones. Furthermore, beamforming—a crucial technique utilized in this context—offers several significant benefits. The directed nature of a beam significantly improves link budgets, thereby enhancing network performance as a whole. In addition, beamforming effectively mitigates inter-port interference, contributing to the antenna system's overall effectiveness and dependability. Overall, this result demonstrates that beamforming has the potential to be an indispensable instrument for improving the performance and functionality of antennas in practical applications.

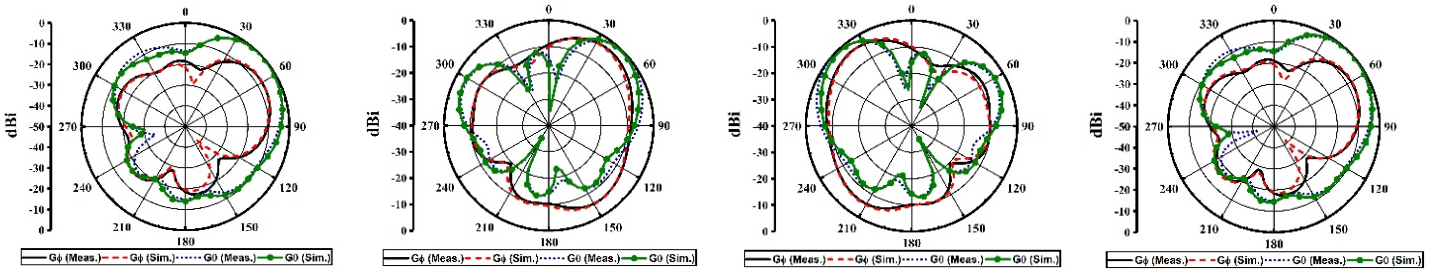

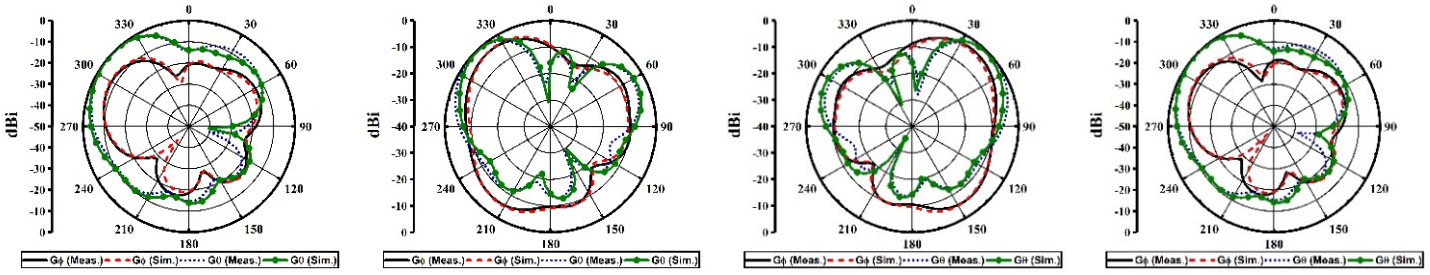

Fig. 11. Normalized radiation pattern at 5.2 GHz: (a) Port-1, (b) Port-2, (c) Port-3, and (d) Port-4.

Fig. 12 depicts the distribution of the electric (E-field) and magnetic (H-field) co mponents on the RDRA. Due to the electrical symmetry of the antenna's structure, the field distribution of only one port is presented despite the fact that it is the same for all ports. The simulated distributions of the electric and magnetic fields at a resonant frequency of 5.2 GHz and a phase angle of 180° are illustrated in Fig. 13. This specific experiment sought to identify the mode in which the proposed antenna design was being stimulated. Fig. 13 shows that the direction of the fields in the RDRA is remarkably similar to that of the Quasi-TM_{111} mode when compared to the matching rectangular resonator mode. The provided top view in the XY plane allowed us to compare them, demonstrating that the direction of the fields is comparable, signifying the influence of the proposed design on mode characteristics. Overall, this analysis provides vital information on the ways in which antenna functions aid in predicting performance and radiation characteristics at a specified frequency.

Table 1 presents the results of a performance assessment of the proposed 3D printable MIMO antenna as compared to existing MIMO RDRAs on the basis of antenna parameters, MIMO characteristics, and antenna size.

V. Conclusion

This study built and investigated a novel four-port MIMO DRA for ISM band applications. Each RDRA was made directional using reflector plates, thus enhancing port isolation, and the antenna was fed through coaxial cables. The proposed antenna achieved a bandwidth of 3 GHz (3.6–6.6 GHz) and a radiation gain above 5.5 dBi across the entire resonance range.

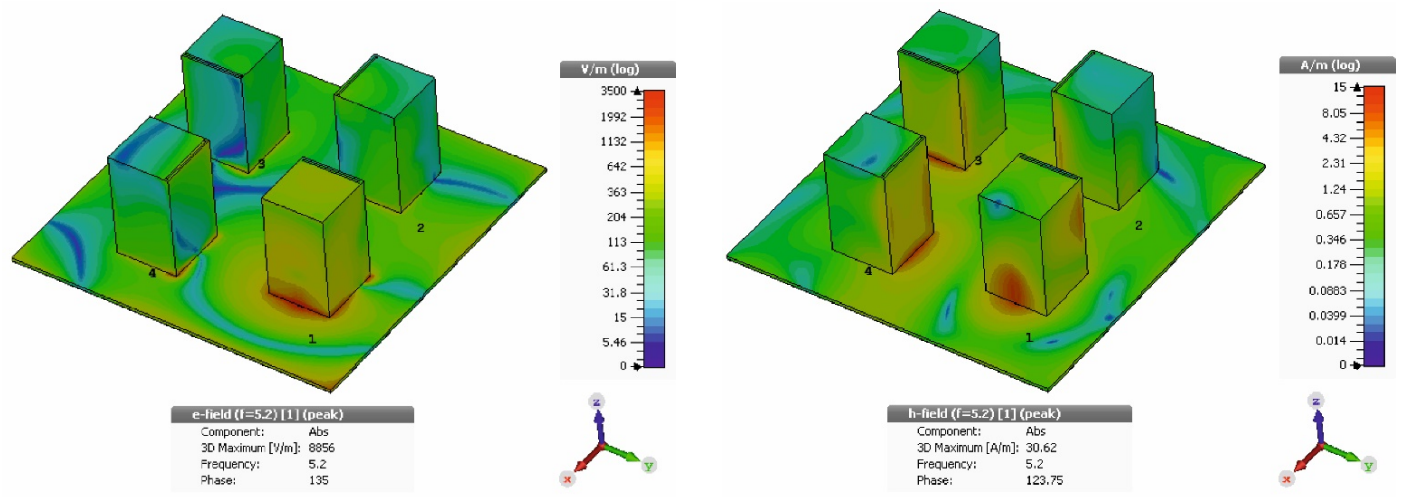

(a) (b)

Fig. 12. Distribution of the field magnitude in the RDRA at 4 GHz: (a) E-field and (b) H-field.

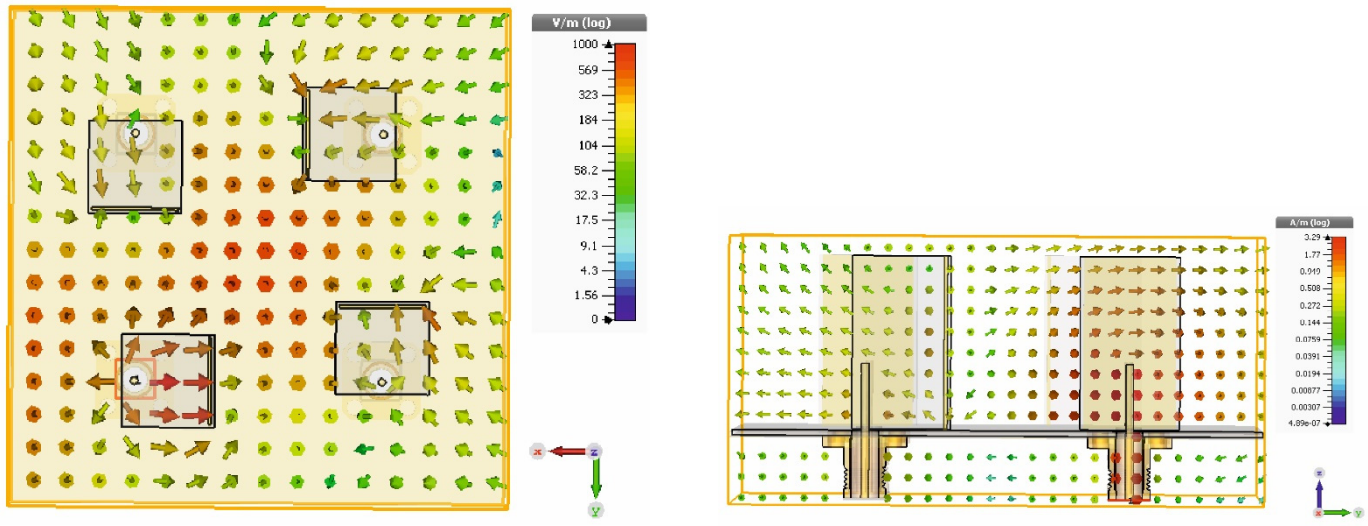

(a) (b)

Fig. 13. Distribution of the fields in the RDRA at 5.2 GHz: (a) E-field and (b) H-field.

Table 1. Performance assessment results

Study	Size (mm)	Bandwidth (GHz)	Isolation (dB)	Gain (dBi)	ρ	G_{app} (dB)
Selvaraju et al. [12]	80×120×29	1.617–2.109 (0.497)	−17	3.2 (1.8 GHz)	0.003 (1.8 GHz)	9.9 (1.8 GHz)
Nasir et al. [13]	80×80×6	2.56–2.64 (0.08)	<−20	N/A	0.054 (2.6 GHz)	9.68 (2.6 GHz)
Proposed	80×80×26	3.6–6.6 (3)	<−25	>5.5 dBi	0.004 (5.1 GHz)	10 (5.1 GHz)

Furthermore, since the antenna was combined with its substrate by employing 3D printing, mounting mistakes were practically non-existent, thus exhibiting increased mechanical robustness.

REFERENCES

[1] S. Dubal and A. Chaudhari, "Mechanisms of reconfigurable antenna: a review," in *Proceedings of 2020 10th International Conference on Cloud Computing, Data Science & Engineering (Confluence)*, Noida, India, 2020, pp. 576-580. https://doi.org/10.1109/Confluence47617.2020.9057998

[2] D. Manteuffel and R. Martens, "Compact multimode multielement antenna for indoor UWB massive MIMO," *IEEE Transactions on Antennas and Propagation*, vol. 64, no. 7, pp. 2689-2697, 2016. https://doi.org/10.1109/TAP.2016.2537388

[3] J. B. Yan and J. T. Bernhard, "Design of a MIMO dielectric resonator antenna for LTE femtocell base stations," *IEEE Transactions on Antennas and Propagation*, vol. 60, no. 2, pp. 438-444, 2012. https://doi.org/10.1109/TAP.2011.2174021

[4] L. Zou, D. Abbott, and C. Fumeaux, "Omnidirectional cylindrical dielectric resonator antenna with dual polarization," *IEEE Antennas and Wireless Propagation Letters*, vol. 11, pp. 515-518, 2012. https://doi.org/10.1109/LAWP.2012.2199277

[5] Y. He, T. Liu, X. Du, and W. Wu, "The design of a tripolarization rectangle dielectric resonator antenna," in *Proceedings of 2016 10th European Conference on Antennas and Propagation (EuCAP)*, Davos, Switzerland, 2016, pp. 1-3. https://doi.org/10.1109/EuCAP.2016.7481834

[6] A. Abdalrazik, A. S. Abd El-Hameed, and A. B. Abdel-Rahman, "A three-port MIMO dielectric resonator antenna using decoupled modes," *IEEE Antennas and Wireless Propagation Letters*, vol. 16, pp. 3104-3107, 2017. https://doi.org/10.1109/LAWP.2017.2763426

[7] M. S. Sharawi, S. K. Podilchak, M. U. Khan, and Y. M. Antar, "Dual-frequency DRA-based MIMO antenna system for wireless access points," *IET Microwaves, Antennas & Propagation*, vol. 11, no. 8, pp. 1174-1182, 2017. https://doi.org/10.1049/iet-map.2016.0671

[8] A. Dadgarpour, B. Zarghooni, B. S. Virdee, T. A. Denidni, and A. A. Kishk, "Mutual coupling reduction in dielectric resonator antennas using metasurface shield for 60-GHz MIMO systems," *IEEE Antennas and Wireless Propagation Letters*, vol. 16, pp. 477-480, 2017. https://doi.org/10.1109/LAWP.2016.2585127

[9] R. Karimian, A. Kesavan, M. Nedil, and T. A. Denidni, "Low-mutual-coupling 60-GHz MIMO antenna system with frequency selective surface wall," *IEEE Antennas and Wireless Propagation Letters*, vol. 16, pp. 373-376, 2017. https://doi.org/10.1109/LAWP.2016.2578179

[10] A. Petosa, *Dielectric Resonator Antenna Handbook*. Norwood, MA: Artech House, 2007.

[11] P. Kumar, S. Dwari, S. Singh, A. Kumar, N. K. Agrawal, and U. Kumar, "Analysis and optimization of conformal patch excited wideband DRA of several shapes," *Frequenz*, vol. 72, no. 5-6, pp. 197-208, 2018. https://doi.org/10.1515/freq-2017-0039

[12] R. Selvaraju, M. R. Kamarudin, M. Khalily, M. H. Jamaluddin, and J. Nasir, "Dual-port MIMO rectangular dielectric resonator antenna for 4G-LTE application," *Applied Mechanics and Materials*, vol. 781, pp. 24-27, 2015. https://doi.org/10.4028/www.scientific.net/AMM.781.24

[13] J. Nasir, M. H. Jamaluddin, M. Khalily, M. R. Kamarudin, and I. Ullah, "Design of an MIMO dielectric resonator antenna for 4G applications," *Wireless Personal Communications*, vol. 88, pp. 525-536, 2016. https://doi.org/10.1007/s11277-016-3174-3

[14] B. Kovacs, A. Geczy, G. Horvath, I. Hajdu, and L. Gal, "Advances in producing functional circuits on biodegradable PCBs," *Periodica Polytechnica Electrical Engineering and Computer Science*, vol. 60, no. 4, pp. 223-231, 2016. https://doi.org/10.3311/PPee.9690

[15] A. Geczy, M. Kovacs, and I. Hajdu, "Conductive layer deposition and peel tests on biodegradable printed circuit boards," in *Proceedings of 2012 IEEE 18th International Symposium for Design and Technology in Electronic Packaging (SIITME)*, Alba Iulia, Romania, 2012, pp. 139-142. https://doi.org/10.1109/SIITME.2012.6384363

[16] N. Ghuttora, "Increase the usage of biopolymers and biodegradable polymers for sustainable environment," Master's thesis, Arcada University of Applied Sciences, Helsinki, Finland, 2016.

[17] N. A. A. B. Taib, M. R. Rahman, D. Huda, K. K. Kuok, S. Hamdan, M. K. B. Bakri, M. R. M. B. Julaihi, and A. Khan, "A review on poly lactic acid (PLA) as a biodegradable polymer," *Polymer Bulletin*, vol. 80, pp. 1179-1213, 2023. https://doi.org/10.1007/s00289-022-04160-y

[18] P. Kumar, S. Dwari, J. Kumar, A. Kumar, and S. Singh, "Investigation of compact dielectric monopole antenna

integrated with 3D printed horn for UWB applications," *Frequenz*, vol. 72, no. 11-12, pp. 489-501, 2018. https://doi.org/10.1515/freq-2017-0273

[19] P. Kumar, S. Dwari, and J. Kumar, "Design of biodegradable quadruple-shaped DRA for WLAN/Wi-Max applications," *Journal of Microwaves, Optoelectronics and Electromagnetic Applications*, vol. 16, pp. 867-880, 2017. https://doi.org/ 10.1590/2179-10742017v16i31019

Rasika Verma

https://orcid.org/0009-0008-6330-178X

received her M.Tech. degree in Digital Communication from Dr. A. P. J. Abdul Kalam University, Lucknow, India. She holds a B.Tech. degree in Electronics and Instrumentation Engineering. Currently, she is pursuing a Ph.D. in Electronics and Communication Engineering from SRM Institute of Science & Technology, Delhi NCR Campus, Ghaziabad, India. Her fields of interest include antenna theory and design as well as RF, microwave, and cloud computing.

Rohit Sharma

https://orcid.org/0000-0002-1600-5039

is an associate professor in the Department of Electronics and Communication Engineering, SRM Institute of Science and Technology, Delhi NCR Campus, Ghaziabad, India. He is an active member of ISTE, IEEE, ICS, IAENG, and IACSIT. He is also an editorial board member and a reviewer of more than 12 international journals and conferences, including *IEEE Access* and *the IEEE Internet of Things Journal.* He has served as a book editor for 7 different titles published by CRC Press, Apple Academic Press, Springer, and Taylor & Francis Group, USA, among others. He received the Young Researcher Award in the 2nd Global Outreach Research and Education Summit & Awards 2019 hosted by the Global Outreach Research & Education Association (GOREA).